

# Multi-scale model of gradient evolution in turbulent flows

Luca Biferale,<sup>1</sup> Laurent Chevillard,<sup>2</sup> Charles Meneveau,<sup>2</sup> and Federico Toschi<sup>3</sup>

<sup>1</sup>*Dip. Fisica and INFN, Università di “Tor Vergata” Via della Ricerca Scientifica 1, 00133 Roma, Italy.*

<sup>2</sup>*Department of Mechanical Engineering and Center for Environmental and Applied Fluid Mechanics, The Johns Hopkins University, 3400 N. Charles Street, Baltimore, MD 21218, USA*

<sup>3</sup>*Istituto per le Applicazioni del Calcolo CNR, Viale del Policlinico 137, 00161 Roma, Italy and INFN, Sezione di Ferrara, Via G. Saragat 1, I-44100 Ferrara, Italy.*

(Dated: November 14, 2017)

A multi-scale model for the evolution of the velocity gradient tensor in fully developed turbulence is proposed. The model is based on a coupling between a “Restricted Euler” dynamics [P. Vieillefosse, *Physica A*, **14**, 150 (1984)] which describes gradient self-stretching, and a deterministic cascade model which allows for energy exchange between different scales. We show that inclusion of the cascade process is sufficient to regularize the well-known finite time singularity of the Restricted Euler dynamics. At the same time, the model retains topological and geometrical features of real turbulent flows: these include the alignment between vorticity and the intermediate eigenvector of the strain-rate tensor and the typical teardrop shape of the joint probability density between the two invariants,  $R - Q$ , of the gradient tensor. The model also possesses skewed, non-Gaussian longitudinal gradient fluctuations and the correct scaling of energy dissipation as a function of Reynolds number. Derivative flatness coefficients are in good agreement with experimental data.

PACS numbers:

The spatio-temporal fluctuations of small-scales in three-dimensional turbulent flows are among the most complex phenomena known to classical physics, being both highly non-Gaussian and strongly long-range correlated. For example, velocity gradients as well as velocity increments between two points typically show strong fluctuations much larger than their standard deviation [1, 2]. The same is true for fluid accelerations or velocity increments at two different times [2, 3, 4], with long-range correlations up to the time scales of the largest eddies in the flow [5]. A possible mechanism for the large fluctuations is the nonlinear self-stretching [6, 7] that occurs during the Lagrangian evolution of the velocity gradients,  $A_{ij} = \partial_i u_j$ . This local self-stretching must be coupled with the energy exchange among larger/smaller eddies and with velocity fluctuations at different spatial locations via the pressure term. The non-linear coupling among different scales also relates to the concept of energy cascade, often invoked to explain the growth of non-Gaussianity going from large to small scales.

Significant advances in experimental techniques now allow to measure all components of  $\mathbf{A}$  in different spatial locations [8, 9, 10] in high Reynolds number flows. These experimental measurements, together with data generated using direct numerical simulations, has uncovered the existence of many interesting, and possibly universal, geometric features of  $\mathbf{A}$ . Namely, (i) the preferred alignment of the vorticity vector with the eigenvector of the intermediate eigenvalue of the strain-rate tensor,  $\mathbf{S} = (\mathbf{A} + \mathbf{A}^T)/2$ ; (ii) the axisymmetric character of local deformation (two positive and one negative eigenvalue of  $\mathbf{S}$ ); (iii) the typical teardrop shape of the joint probability distribution,  $P(R, Q)$  where  $R = -\text{Tr}(\mathbf{A}^3)/3$  and  $Q = -\text{Tr}(\mathbf{A}^2/2)$  are two invariants of  $\mathbf{A}$  [7, 8, 11, 12, 13].

A systematic analysis of the dynamics of velocity gradients was made by Vieillefosse [6]. He started from the exact equations governing the Lagrangian evolution of  $\mathbf{A}$  in the incompressible Navier-Stokes (NS) equations:  $\frac{d}{dt} A_{ij} = -A_{ik} A_{kj} - \partial_i \partial_j p + \nu \partial^2 A_{ij}$ , where  $p$  is the pressure divided by density,  $\nu$  is the kinematic viscosity and with  $d/dt$  we mean the Lagrangian derivative. Then, he retained only the isotropic part of the pressure Hessian,  $\partial_i \partial_j p \sim \delta_{ij} \partial^2 p$  and used the incompressibility condition to express the pressure Laplacian in terms of  $\mathbf{A}$ . Finally he neglected the viscous contribution arriving to the closed “Restricted Euler” (RE) equations:

$$\frac{d}{dt} \mathbf{A} = -\mathbf{A}^2 + \text{Tr}(\mathbf{A}^2) \mathbf{I}/3. \quad (1)$$

It is remarkable that such a simple system is already sufficient to explain many of the geometrical trends found in the real gradient evolution, as shown by [6, 7]. On the other hand, the self-stretching mechanism is not constrained by any energy exchange/loss mechanism, leading to a finite time singularity for any initial condition. This blow up prevents the use of the RE dynamics to make any systematic assessment of the gradient’s stationary statistics. Prior models that seek to regularize the RE dynamics include a stochastic model with log-normal statistics of the dissipation [15], a linear and non-linear damping model for the viscous term [16], and a model where the material deformation history described by a tetrad of points plus some stochastic terms are used to mimic the anisotropic pressure fluctuations [13]. Recently, a model of the anisotropic pressure Hessian and of the viscous term has been proposed by introducing a finite-time memory effect in the closure of the material deformation tensor [17]. Results show that this model re-

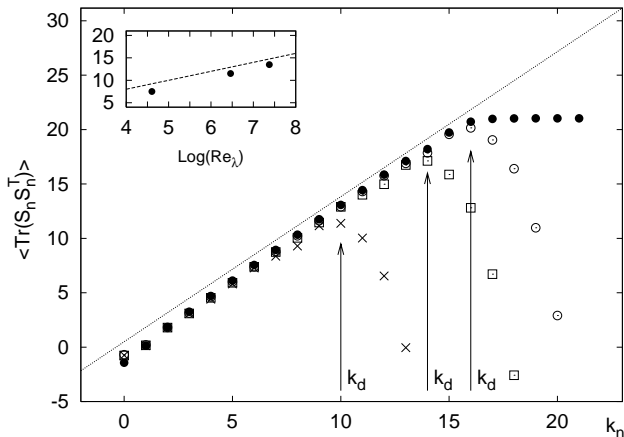


FIG. 1: Log-log plot of the mean energy dissipation (divided by  $2\nu$ ):  $\langle \text{Tr}(\mathbf{S}_n \mathbf{S}_n^T) \rangle$  versus  $k_n$ , for  $Re_\lambda = 1,500$  ( $\circ$ );  $Re_\lambda = 600$  ( $\square$ );  $Re_\lambda = 130$  ( $\times$ ). The dissipative scale  $k_d$  is defined as the wavenumber where the energy dissipation peaks (arrows in the plot). The straight line correspond to the Kolmogorov spectrum  $\sim k_n^{4/3}$ . The data which saturates in the viscous range,  $\bullet$ , are for the coarse-grained (defined later in the text) variables:  $\langle \text{Tr}(\mathbf{S}_n^{CG} \mathbf{S}_n^{CGT}) \rangle$ . In the inset we show the Reynolds dependency of the energy dissipation evaluated at  $k_d$ . The straight line corresponds to the expected slope  $\propto Re_\lambda^2$ .

produces stationarity, non-Gaussianity of transverse and longitudinal gradients and the correct geometrical properties of  $\mathbf{A}$ . Remarkably, the system also predicts experimentally observed relative scaling exponents characterizing how non-Gaussian statistics evolves with Reynolds number, at least from small to moderate values of it. However, attempts to simulate velocity gradient dynamics at arbitrarily large Reynolds numbers with this model have been, so far, unsuccessful. It was concluded that the difficulties were associated to the assumptions that the velocity gradient tensor evolves mainly uncoupled from larger/smaller eddies and neighboring locations. In this paper we propose a minimal model in which deterministic couplings among scales of motion are included. The model couples the self-stretching local dynamics *à la* Vieillefosse with a cascade mechanism, i.e. by coupling the velocity evolution on the gradient scale given by (1) with velocity fluctuations at larger scales. The most remarkable result is that such a coupling will be shown to be sufficient to regularize the Vieillefosse finite-time singularity, without destroying the main positive features of (1) including the presence of skewed longitudinal gradients and long tails in the probability density functions of gradients; the vorticity alignment and the typical teardrop shape of the joint probability,  $P(R, Q)$ . Also the intermittency level as measured by the flatness coefficient is in good quantitative agreement with experiments [1, 20]. The model thus provides meaningful results even for very large Reynolds number (here we present results

up to  $Re_\lambda = 1,500$ ).

To introduce a cascade dynamics we start from a decomposition of the gradient tensor into band-passed contributions  $\mathbf{A} = \sum_n \mathbf{A}_n$ , each  $\mathbf{A}_n$  describes the velocity gradient at a typical wavenumber  $k_n$  [18]. The set of possible wavenumbers is chosen equispaced on a logarithmic scale,  $k_n = 2^n k_0$ , such as to optimally capture power-law behaviors in the inertial range. The band-passed version of the NS equations is of the form

$$\frac{d}{dt} \mathbf{A}_n = - \sum_{p,q} (\mathbf{A}_p \mathbf{A}_q)_n + \mathbf{B}_n - \frac{\text{Tr}(\%)}{3} \mathbf{I} + \nu \partial^2 \mathbf{A}_n, \quad (2)$$

where the trace term is added to keep the entire right-hand-side trace-free, and the term  $\mathbf{B}_n$  represents pressure effects, interscale interactions and additional spatial transport introduced by the band-pass filtering acting on the advective term on the left side of the original equation. Neglecting the viscous term and  $\mathbf{B}_n$ , and keeping only the fully diagonal term ( $p = q = n$ ) in the double sum leads to the most severe approximation. Namely that the gradients,  $\mathbf{A}_n$ , band-passed on different shells, follow the RE dynamics separately shell-by-shell:  $d\mathbf{A}_n/dt = -\mathbf{A}_n^2 + 1/3 \text{Tr}(\mathbf{A}_n^2) \mathbf{I}$ . Of course this set of uncoupled equations suffers from the same drawbacks of the original Vieillefosse model. The coupling between different scales must be introduced by keeping some terms besides the purely diagonal one in the first term in the rhs of Eq. 2: i.e. we include a new term  $F$  and we choose its form by imposing an energy preserving structure for the coupling terms, following the assumption that the pressure-Hessian does not perform work on the band-passed gradient [13]. Moreover, it is natural to suppose that the most relevant dynamical interactions happen within nearby scales, (locality assumption) and therefore we limit the range of interactions to the next-nearest neighbors (up to  $n \pm 2$ , for each  $k_n$ ). One possible choice for the coupling term on the  $n$ th shell is:

$$\mathbf{F}_n[A, A] = \mathbf{A}_{n+2} \mathbf{A}_{n+1}^T + b^2 \mathbf{A}_{n-1}^T \mathbf{A}_{n+1} + (1-b)^2 \mathbf{A}_{n-2} \mathbf{A}_{n-1} - \text{Tr}[\%], \quad (3)$$

where  $b$  is a free parameter (always fixed to  $b = 0.5$  hereafter). Let us notice that the structure of  $\mathbf{F}_n[A, A]$  is chosen such that the total energy  $E = \sum_n k_n^{-2} \text{Tr}(\mathbf{A}_n \mathbf{A}_n^T)$  is preserved by the effects of the three nonlinear terms. The model form is proposed as a model for the neglect of all the truncated terms in the double sum and the  $\mathbf{B}_n$  transport term. The functional form proposed for  $\mathbf{F}_n[A, A]$  is motivated by the typical structure of the nonlinear terms used in Shell models of turbulence [14], with the important difference that via (3) we can access now the whole geometrical properties of the band-passed variables, owing to the tensorial structure of the  $\mathbf{A}_n$  variables. To introduce a characteristic wavenumber from which the gradient variables receive their maximal contribution, we

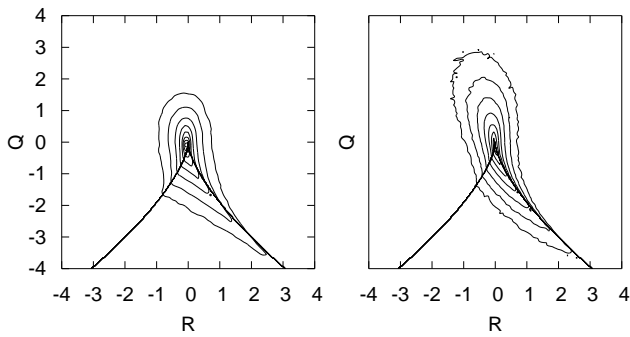


FIG. 2: Isolines of  $P(R, Q)$  for DNS and model data. Right panel: DNS data at  $Re_\lambda \sim 180$ . Left panel: model data at  $Re_\lambda = 140$ , evaluated at the dissipative scale  $k_d(Re)$ . The continuous line in all diagrams correspond to the Vieillefosse zero-discriminant curve  $Q^3 + 27/4R^2 = 0$ .

need a viscous damping. The simplest dimensionally consistent way to do this is by modeling the viscous Laplacian term in NS equations using a linear damping term on each band proportional to  $\nu k_n^2$ , where  $\nu$  is the viscosity. Combining all these elements one obtains the following dynamical system:

$$\frac{d\mathbf{A}_n}{dt} = \alpha \left[ -\mathbf{A}_n^2 + \frac{1}{3}\text{Tr}(\mathbf{A}_n^2)\mathbf{I} \right] + (1 - \alpha) (\mathbf{F}_n - \nu k_n^2 \mathbf{A}_n) \quad (4)$$

where  $\alpha$  is a parameter which weights the relative importance of the RE dynamics with respect to the energy exchange and energy dissipation terms. As a first step, in this work we restrict attention to the case  $\alpha = 0.5$ . The system consist of  $9N$  coupled nonlinear equations. In the previous equations the infrared and ultraviolet truncation is imposed by keeping in the nonlinear term  $A_n = 0$  for  $n = \{-1, -2, N + 1, N + 2\}$ .

The main question we want to answer now is if a stationary statistical state can be achieved once a forcing is applied at large scales. In other words, we want to understand if the simple energy-exchange term,  $\mathbf{F}_n[A, A]$ , is sufficient to regularize the dynamics of the RE structure at all scales. Hopefully, this will allow us also to study the important questions related to the dependency of geometrical structure of turbulence on the Reynolds numbers and its correlation with inertial range quantities. The simplest way to achieve a stationary state is to add a white-in-time Gaussian variable,  $\mathbf{G}$ , at the largest band,  $n = 0$ , where in order to satisfy the requirements of homogeneity and isotropy, we must chose the covariance of the forcing to be  $\langle G_{ij}G_{ml} \rangle = 2\delta_{im}\delta_{jl} - 1/2\delta_{ij}\delta_{ml} - 1/2\delta_{il}\delta_{jm}$  [17].

The gradient statistics will be studied by looking at the

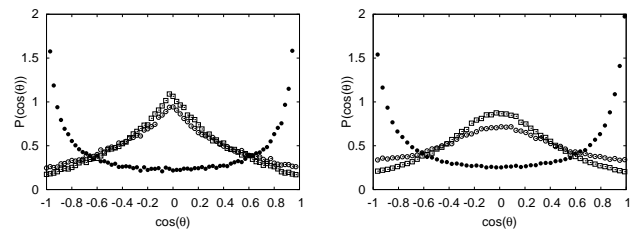


FIG. 3: PDF of the cosine between the vorticity and the eigenvectors associated with the Intermediate (+), maximum (\*) and smallest (x) eigenvalues of the strain-rate matrix. Notice the good agreement between the DNS (right) data and the model data (left).

shell  $k_d$  (where  $n = d$ ), defined as where the spectrum of the  $\mathbf{A}_n$  has its peak, i.e. where a balance between the quadratic terms and the viscous terms of (4) is obtained. The system of equations is integrated numerically using a 4-th order Runge-Kutta scheme. Three Reynolds numbers are simulated by using viscosities equal to  $\nu = \{10^{-4}, 2.7 \times 10^{-6}, 4.4 \times 10^{-7}\}$  and with a total number of shells  $N = \{14, 18, 22\}$ , corresponding to  $Re_\lambda = \{130, 640, 1, 500\}$  respectively. Results are shown in Fig 1, which shows the time-averaged energy dissipation (without multiplication by  $\nu$ ), measured on the band-pass gradient variables,  $\langle \text{Tr}(\mathbf{A}_n \mathbf{A}_n^T) \rangle$  as function of  $k_n$ : notice that it has the expected Kolmogorov scaling  $\langle \text{Tr}(\mathbf{A}_n \mathbf{A}_n^T) \rangle \sim \langle \text{Tr}(\mathbf{S}_n \mathbf{S}_n^T) \rangle \sim k_n^{4/3}$ . On dimensional grounds we expect that the wavenumber where the matching is achieved scales with Reynolds number as  $k_d \sim Re_\lambda^2$ . This is indeed verified in the inset of Fig (1). Geometrical properties of small-scale turbulent fluctuations can be monitored by studying the joint statistics of the two invariants,  $Q, R$  at different Reynolds number and/or at different scales. Here, by measuring the simultaneous distribution of  $Q_n = \text{Tr}(\mathbf{A}_n^2)$  and of  $R_n = \text{Tr}(\mathbf{A}_n^3)$  for different Reynolds numbers we can do both. In Fig (2) we show the isolines of the joint probability distribution  $P(R_n, Q_n)$  measured on the dissipative scale  $n = d$ . We notice the presence of high probable fluctuations along the right Vieillefosse tail, also seen in real turbulence, which is shown in the same figure panel (b). The data are from direct numerical simulation (DNS), done at a similar Reynolds number. As can be seen, there is very good agreement of the model with the Navier-Stokes data, except for a small depletion of events in the third quadrant ( $R < 0, Q > 0$ ). In this quadrant, real data are strongly affected by vortex stretching, an effect which is evidently under-represented by the model evolution. The  $P(R, Q)$  distribution has very little sensitivity to Reynolds number (at least in the range investigated here). The  $P(R, Q)$  distribution becomes more symmetric for band-pass variables at larger scales (not shown), and this effect is also observed in Navier-Stokes

turbulence [12, 13]. Finally, in Fig. (3) we present quantification of the alignment between the vorticity at the dissipative scale,  $(w_i)_d = \epsilon_{ijl}(A_{jl})_d$ , and the three eigenvectors of the strain rate tensor  $\mathbf{S}_d$  also at that scale. It is well-known from DNS and experiments that vorticity tends to preferentially align with the intermediate eigenvector [8, 9, 19]: Figure (3) shows that our model is able to capture also this feature. Finally, we document the results in terms of intermittency. First, we show in the inset of Fig (4) the pdf of both longitudinal and transverse gradients. Correctly, the model possesses longitudinal skewed distribution while the transverse gradient pdf is fully symmetric. The gradient fluctuations are highly non-Gaussian, as a results of the growth of intermittency going from the large scale down to the dissipative scale. The growth of intermittency at decreasing length scales is often characterized by measuring the flatness coefficient of velocity gradients,  $F_4 = \langle A_d^4 \rangle / \langle A_d^2 \rangle^2$  and plotting it as function of Reynolds number  $Re_\lambda$ , where with  $A_d$  we mean any of the longitudinal components of  $\mathbf{A}$ . As a technical difficulty we point out that the exponential fall-off of the gradient spectrum in the shell-matrix model (4) prevents us from a direct measurement of  $F_4$  on the dissipative shell (the flatness tends to grow exponentially in the dissipative range, making the estimate very delicate). For that reasons we decide to measure the flatness using a coarse-grained variable. Specifically, the coarse-grained velocity gradient at scale  $k_m$  is defined as  $A_m^{CG} = \sum_{n=0}^{n=m} A_n$ . For large  $m$ , we obtain a variable which includes fluctuations on all scales, and which becomes independent on  $m$  (saturates) beyond the viscous range. The two variables  $A_n$  and  $A_n^{CG}$  have obviously the same scaling in the inertial range; in the dissipative range the band-passed decays exponentially while the coarse-grained saturates, see Fig (1). This saturation allows us to have robust measurements of intermittency in the dissipative range. In the main body of Fig. (4) we show the behaviour of Flatness of the coarse-grained velocity gradient as a function of Reynolds number, superposed with experimental data. Within the range of Reynolds numbers considered, the agreement is very satisfactory.

In conclusion, we have introduced a “shell” version of the RE dynamics which is free from the finite time singularity of the original Vieillefosse formulation. The regularization is achieved at all scales thanks to the introduction of an energy-exchange mechanism with smaller and larger eddies. A viscous dissipative term is introduced which acts preferentially at the viscous scale where the gradients peak. The model shows very realistic behavior at changing Reynolds numbers, including (i) the skewed nature of longitudinal gradients, (ii) the alignment of vorticity with the intermediate eigenvector of the strain rate tensor, (iii) the accumulation of events along the right tail of the Vieillefosse line and (iv) the correct level of intermittency as measured by the Flatness and its increasing trend at increasing  $Re_\lambda$ . A set of

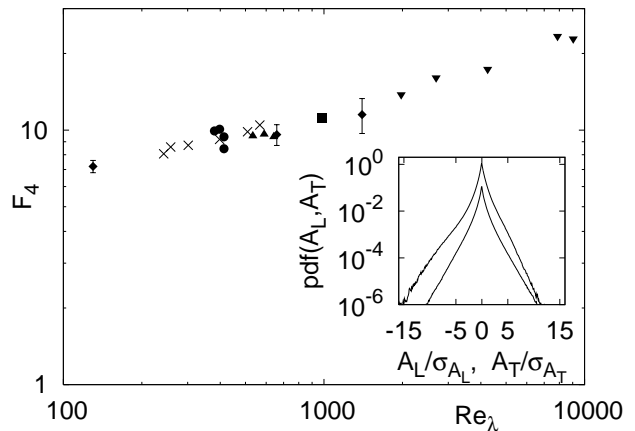


FIG. 4: Comparison between a collection of experimental data for the longitudinal gradient flatness [20], superposed with the results from our model (diamonds with error bars). Where we have used the variance of the longitudinal coarse grained gradient,  $\sigma_A = \langle (A_{11}^{CG})^2 \rangle^{1/2}$ , to define the Reynolds number:  $Re_\lambda = 2E/(3\nu\sigma_A)$  [2]. Inset: Data for  $Re_\lambda = 1500$ . Normalized Pdf of longitudinal (top) and transverse (bottom) band-passed gradients measured at  $k_d$ . Notice the skewed profile for the longitudinal gradients. Longitudinal pdf has been shifted along the y-axis for sake of clarity.

questions remains open. From a dynamical point of view, the model seems to under-predict the probability of observing strong vortex stretching events - this could point to open challenges associated with modeling small-scale coherent vortices [4]. From a statistical point of view, it will be interesting to explore the effects of varying the free parameters  $\alpha$  and  $b$  on intermittency levels. The free parameter  $\alpha$  defines the relative importance of the local Vieillefosse dynamics with respect to the energy exchange mechanism. A promising development could be to couple the present multi-scale approach with the Lagrangian deformation method proposed in [17], which proved to be successful in reproducing the main features of turbulent gradients at small and moderate Reynolds.

We thank R. Benzi for helpful discussions. L.B. and F.T. acknowledge the hospitality of the Center for Environmental and Applied Fluid Mechanics of Johns Hopkins University where part of this work has been done. L.C. acknowledges the support of the Keck Foundation, C.M. thanks the support of the US National Science Foundation, F.T. thanks CNR for support under the Short Term Mobility grant.

- 
- [1] K.R. Sreenivasan and R. Antonia, *Annu. Rev. Fluid Mech.* **29** 435 (1997).
  - [2] U. Frisch, *Turbulence: the legacy of A.N. Kolmogorov* (Cambridge University Press, Cambridge, 1995).
  - [3] La Porta et al. *Nature* **409**, 1017 (2001); *J. Fluid*

- Mech.* **469**, 121 (2002).
- [4] L. Biferale et al. *Phys. Fluids*. **17**, 021701 (2005); L. Chevillard et al., *Phys. Rev. Lett.* **91**, 214502 (2003).
- [5] N. Mordant, E. Leveque and J-F. Pinton, *New Journal of Physics* **6** 116 (2004).
- [6] P. Vieillefosse, *Physica A* **125** 150 (1984).
- [7] B.J. Cantwell, *Phys. Fluids A* **5**, 2008 (1993); *Phys. Fluids A* **4**, 782 (1992)
- [8] A. Tsinober, E. Kit and T. Dracos, **242** 169 (1992); B. Luthi, A. Tsinober and W. Kinzelbach, *J. Fluid Mech.* **528** 87 (2005).
- [9] B. Tao, J. Katz & C. Meneveau *J. Fluid Mech.* **467** 35 (2002).
- [10] B.W. Zeff et al., *Nature* **421** 146 (2003).
- [11] T.S. Lund and M.M. Rogers, *Phys Fluids* **6** 1838 (1994).
- [12] F. van der Bos et al., *Phys Fluids* **14** 2457 (2002).
- [13] M. Chertkov, A. Pumir and B. Shraiman, *Phys. Fluids* **11** 2394 (1999); A. Naso and A. Pumir, *Phys. Rev. E* **72** 056318 (2005).
- [14] L. Biferale, *Annu. Rev. Fluid Mech.* **35** 441 (2003).
- [15] S.S. Girimaji and S.B. Pope, *Phys Fluids A* **2** 242 (1990).
- [16] J. Martin et al., *Phys. Fluids* **10** 2336 (1998). E. Jeong and S. S. Girimaji, *Theor. Comput. Fluid Dyn.* **16**, 421 (2003).
- [17] L. Chevillard and C. Meneveau, *Phys. Rev. Lett* **97**, 174501 (2006).
- [18] G. Eyink, *J. Fluid Mech.* **549**, 159 (2006).
- [19] W.T. Ashurst et al., *Phys. Fluids* **30**, 2343 (1987).
- [20] R. A. Antonia, A. J. Chambers, and B. R. Satyaprakash *Boundary-Layer Meteorology* **21** (1981) 159-171.